JLB

Article

RLR-mediated production of interferon-β by a human dendritic cell subset and its role in virus-specific immunity

Attila Szabo, Krisztián Bene,* Péter Gogolák,* Bence Réthi,*,† Árpád Lányi,* István Jankovich,‡ Balázs Dezső,§ and Éva Rajnavölgyi*,1*

Departments of *Immunology and §Pathology, Medical and Health Science Centre, University of Debrecen, Debrecen, Hungary; †Department of Microbiology, Tumor and Cell Biology, Karolinska Institute, Stockholm, Sweden; and ‡National Center for Epidemiology (NCE), Budapest, Hungary

RECEIVED JULY 18, 2011; REVISED MARCH 29, 2012; ACCEPTED MARCH 30, 2012. DOI: 10.1189/jlb.0711360

ABSTRACT

Cytosolic RIG-I-like helicases (RLR) are PRRs involved in type I IFN production and antiviral immunity. This study focuses to the comparison of the expression, function, and signaling cascades associated to RLR in the previously identified $CD14^-$DC-$SIGN^+PPAR\gamma^{low}CD1a^+$ and $CD14^{low}$DC-$SIGN^+PPAR\gamma^{high}CD1a^-$ human moDC subsets. Our results revealed that the expression of RLR genes and proteins as well as the activity of the coupled signaling pathways are significantly higher in the $CD1a^+$ subset than in its phenotypically and functionally distinct counterpart. Specific activation of RLR in moDCs by poly(I:C) or influenza virus was shown to induce the secretion of IFN-β via IRF3, whereas induction of proinflammatory cytokine responses were predominantly controlled by TLR3. The requirement of RLR-mediated signaling in $CD1a^+$ moDCs for priming naïve $CD8^+$ T lymphocytes and inducing influenza virus-specific cellular immune responses was confirmed by RIG-I/MDA5 silencing, which abrogated these functions. Our results demonstrate the subset-specific activation of RLR and the underlying mechanisms behind its cytokine secretion profile and identify $CD1a^+$ moDCs as an inflammatory subset with specialized functional activities. We also provide evidence that this migratory DC subset can be detected in human tonsil and reactive LNs. *J. Leukoc. Biol.* 92: 159–169; 2012.

Introduction

The heterogeneous population of DCs interacts with many leukocyte types and acts as professional APCs in lymphoid and nonlymphoid tissues [1]. They are considered as coordinators of innate and adaptive immunity and regulators of self-tolerance and immune responses. DCs derive from hematopoietic precursors and are classified to pDCs and cDCs, characterized by different tissue distribution and defense mechanisms. Circulating prepDCs differentiate and become activated in lymphoid tissues and are specialized for the production of high amounts of type I IFNs [2]. Steady-state cDCs derive from a common bone marrow monocyte/DC progenitor, migrate to lymphoid and peripheral tissues, and are replenished from circulating and/or local precursors, respectively [3]. Under inflammatory conditions, circulating monocytes are recruited to inflamed tissues, where they develop to macrophages or moDCs with phagocytic activity and as a result of activation, the expression of costimulatory molecules and the capability to produce cytokines and chemokines [4]. Intense research in the past years revealed the origin and development of multiple DC subsets in mice and man (reviewed in refs. [5, 6]) and linked them to specialized functions, such as migratory potential, secretion of a unique combination of cytokines, or cross-priming $CD8\alpha^+$ CTLs [7].

In vitro-generated human moDCs provide a rich source of cells with remarkable plasticity upon responding to various signals and thus, emerged as promising candidates of various immunotherapies and have been used for targeting vaccines against cancers and viruses [8, 9]. DCs express a wide array of PRRs, which are distributed to various cellular compartments. C-type lectins, FcRs and complement receptors, as well as TLRs are integrated to plasma or vesicular membranes, whereas NLRs and RLRs are cytosolic molecular sensors of foreign and modified nucleotides [10]. cDCs display membrane TLR4 and intracellular TLR3, -7, and -8 [11] and also express cytosolic RLR and NLR [12]. The cell type-specific expression and the intracellular compartmentalization of PRR determine the synergistic or inhibitory cross-talk of these receptors, the

Abbreviations: cDC=classical/conventional DC, H1N1=A/Brisbane/59/7, IF=immunofluorescence, IHC=immunohistochemistry, IP=immunoperoxidase, IRF=IFN regulatory factor, MDA5=melanoma differentiation-associated gene 5, moDC=monocyte-derived DC, NLR=nucleotide-binding oligomerization-like receptor, p=phospho, pDC=plasmacytoid DC, poly(I:C)=polyinosinic:polycytidylic acid, PPARγ=peroxisome proliferator-activated receptor γ, QPCR=quantitative PCR, RIG-I=retinoic acid-induced gene I, RLR=retinoic acid-induced gene I-like receptor, SIGN=specific ICAM-3-grabbing nonintegrin, siRNA=small interfering RNA

The online version of this paper, found at www.jleukbio.org, includes supplemental information.

1. Correspondence: Department of Immunology, Medical and Health Science Centre, University of Debrecen, Debrecen, 1. Egyetem sqr. Debrecen 4032, Hungary. E-mail: evaraj@med.unideb.hu

interplay of the coupled signaling pathways they trigger, and the effector molecules they produce [13].

In our previous studies, we identified two human moDC subsets, which differ in their phenotypic and functional characteristics [14, 15]. The $CD14^{low}$DC-$SIGN^{+}PPAR\gamma^{high}CD1a^{-}$ moDC subset, referred to as $CD1a^{-}$ DC, has been identified throughout LNs and stands out with efficient phagocytosis of bacteria and apoptotic cells [16]. Dependent on environmental cues, these cells develop to $CD14^{-}$DC-$SIGN^{+}PPAR\gamma^{low}CD1a^{+}$ inflammatory cells with high cytokine secretion and membrane expression of CD40 and E-cadherin. This $CD1a^{+}$ DC subset is detectable in the interfollicular areas of reactive LNs [14]. The ratio of $CD1a^{-}$ and $CD1a^{+}$ moDCs varies among individuals and is negatively regulated by serum lipids and synthetic PPARγ ligands [17], which have been shown to ameliorate immune pathology in mice infected by highly pathogenic influenza virus [18]. As the molecular background of the inflammatory nature of $CD1a^{+}$ moDCs has not been analyzed so far, we addressed the questions of whether these DC subsets differ in their capability of sensing viral dsRNA by RLR, and if so, were there any differences in their proinflammatory and type I IFN responses.

We showed that RIG-I and MDA5 gene and protein expressions are significantly higher in $CD1a^{+}$ moDCs than in their $CD1a^{-}$ counterpart, and components of the RLR-related signaling pathway are also expressed preferentially in the $CD1a^{+}$ subset. The RLR-coupled signaling pathway, triggered by poly(I:C) or influenza virus, is also more active in the $CD1a^{+}$ subset than in $CD1a^{-}$ cells and results in the production of IFN-β in an IRF3-dependent manner. We also provide the first evidence that the type I IFN response in human moDCs is primarily mediated by the RLR sensor system, whereas the regulation of proinflammatory cytokine production is under the control of the TLR3-NF-κB pathway, which challenges the current paradigm concerning the collaborative or dichotomical regulation of type I IFN and inflammatory cytokine responses.

MATERIALS AND METHODS

Cells, flow cytometry, and cell sorting

Leukocyte-enriched buffy coats were obtained from healthy blood donors drawn at the Regional Blood Center of the Hungarian National Blood Transfusion Service (Debrecen, Hungary) in accordance with the written approval of the Director of the National Blood Transfusion Service and the Regional and Institutional Ethics Committee of the University of Debrecen, Medical and Health Science Center (Hungary). Written, informed consent was obtained from the donors' prior blood donation, and their data were processed and stored according to the directives of the European Union. PBMCs were separated by a standard density gradient centrifugation with Ficoll-Paque Plus (Amersham Biosciences, Uppsala, Sweden). Monocytes were purified from PBMCs by positive selection using immunomagnetic cell separation with anti-CD14 microbeads, according to the manufacturer's instruction (Miltenyi Biotec, Bergisch Gladbach, Germany). After separation on a VarioMACS magnet, 96–99% of the cells were $CD14^{+}$ monocytes, as measured by flow cytometry. Monocytes were cultured in 12-well tissue-culture plates at a density of 2×10^{6} cells/ml in AIM-V medium (Invitrogen, Carlsbad, CA, USA), supplemented with 80 ng/ml GM-CSF (Gentaur Molecular Products, Brussels, Belgium) and 100 ng/ml IL-4 (PeproTech EC, London, UK). On Day 2, the same amounts of GM-CSF and IL-4 were added to the cell cultures.

Phenotyping of resting and activated moDCs was performed by flow cytometry using anti-CD83-FITC, anti-CD86-PE, anti-CD1a-PE, and anti-CD14-PE (Beckman Coulter, Hialeah, FL, USA) and anti-HLA-DR-FITC and isotype-matched control antibody (BD PharMingen, San Diego, CA, USA). Fluorescence intensities were measured by FACSCalibur (BD Biosciences, Franklin Lakes, NJ, USA), and data were analyzed by FlowJo software (Tree Star, Ashland, OR, USA). The $CD1a^{+}$ and $CD1a^{-}$ cells were separated with FACSDiva high-speed cell sorter (BD Biosciences). Autologous, naive T cells were separated from mononuclear cells using human naive $CD4^{+}$ and $CD8^{+}$ T cell isolation kits (Miltenyi Biotec).

Activation of DCs

Bacterial LPS (Sigma, Schnelldorf, Germany), ATRA (Sigma), and high molecular-weight poly(I:C) (InvivoGen, San Diego, CA, USA) were used at concentrations indicated in the figure legends. To prepare cell lysates for Western blotting, DCs were activated for 24 h, to collect supernatants for ELISA and prepare cell lysates for QPCR for 18–24 h. Purified live and inactivated H1N1 influenza virus (kindly provided by NCE, Hungary) of 6×10^{6} PFU/mL was used for in vitro treatment of 1×10^{6}/mL sorted DC in serum-free AIM V medium for 24 h.

RNA isolation, cDNA synthesis, and QPCR

Real-time QPCR was performed as described previously [14]. Briefly, total RNA was isolated by TRIzol reagent (Invitrogen). Total RNA (1.5–2 μg) was reverse-transcribed using SuperScript II RNase H RT (Invitrogen) and Oligo(dT)15 primers (Promega, Madison, WI, USA). Gene-specific TaqMan assays (Applied Biosystems, Foster City, CA, USA) were used to perform QPCR in a final volume of 25 μl in triplicates using AmpliTaq DNA polymerase and ABI Prism 7900HT real-time PCR instrument (Applied Biosystems). Amplification of 36B4 and/or cyclophylin were used as normalizing controls. Cycle threshold values were determined using the SDS 2.1 software. Constant threshold values were set for each gene throughout the study. The sequences of the primers and probes are available upon request.

siRNA experiments

Gene-specific siRNA knockdown was performed by SilencerSelect siRNA (Applied Biosystems) transfection at Day 3 of in vitro DC differentiation using Gene Pulser Xcell instrument (Bio-Rad, Hercules, CA, USA). Silencing of helicase genes was performed by RIG-I and MDA5 siRNA mix (BiMix). Silencer negative control nontargeting siRNA (Applied Biosystems) was used as a negative control. The efficacy of siRNA treatments was tested before and after DC activation on Days 5 and 6, respectively, by QPCR and Western blotting.

Western blotting

Cells were lysed in Laemmli buffer, and the protein extracts were tested by antibody specific for TLR3 (Abcam, Cambridge, UK); anti-MDA5 (Lifespan, Seattle, WA, USA); RIG-I, IκB-α, pIκB-α, IRF3, and pIRF3 (Cell Signaling Technology, Danvers, MA, USA); and β-actin (Sigma), diluted to 1:1000; secondary antibodies were used at 1:5000. Anti-rabbit or anti-mouse (pIκB-α) antibody, conjugated to HRP (GE Healthcare, Little Chalfont Buckinghamshire, UK), was used as a secondary antibody. The SuperSignal ECL system was used for probing target proteins (Thermo Scientific, Rockford, IL, USA). After the membranes had been probed for the target protein, they were stripped and reprobed for β-actin.

Cytokine measurements

Culture supernatants of DCs were harvested 18–24 h after activation, and the concentration of IL-6, TNF-α, CXCL10, and IL-12p70 was measured using OptEIA kits (BD Biosciences). The level of secreted IFN-β was measured by a human IFN-β ELISA kit (Cell Sciences, Canton, MA, USA).

IFN-γ ELISPOT assay

Activated DCs (2×10^{5} cells/well) were cocultured with naïve, autologous T cells (10^{6} cells/well) in serum-free AIM V medium for 5 days at 37°C in a humidified atmosphere containing 5% CO_2. PHA and Con A-activated T cells were used as

positive controls; nontreated DC + T cell cocultures and T cells without DC served as negative controls. Detection of cytokine-secreting T cells was performed by the avidin-HRP system (NatuTec GmbH, Germany). Plates were analyzed on an ImmunoScan plate reader (CTL, Shaker Heights, OH, USA).

IHC and IF staining

Immunostaining was performed on human tissues obtained from formalin-fixed and/or paraffin-embedded surgical specimens. RIG-I and MDA5 rabbit polyclonal antibody (Cell Signaling and Lifespan, respectively) were used at a dilution of 1:50. As reference antibody, affinity-purified rabbit antibody:S100 protein (1:1000; Novocastra, Newcastle, UK) was used. Biotin-free EnVision$^+$-HRP system (Dako, Denmark) and Very Intense Purple chromogen (Vector Labs, UK) were used for detection, according to the manufacturer's instructions. Single and double IF staining was performed as described [15]. A tyramide-coupled red fluorescent amplification kit, using tetramethylrhodamine (of the tyramide signal amplification fluorescent system, PerkinElmer Life Sciences, Wellesley, MA, USA) with DAPI (blue fluorescence; Vector Labs) nuclear counterstaining, was used for visualization. For double IF, the first antibody labeling was followed by the second antibody treatment using preformed antibody-biotinylated $(Fab')_2$ complex and streptavidin-FITC fluorochrome (green). To ensure the specificity of immunostainings, isotype-matched control IgG (DakoCytomation, Denmark) was used. The topographic identities of immunostained S100-positive DCs were determined on serial sections of reactive LNs in parallel with intracellular RIG-I and MDA5 expression, and the double-immunolabeled samples served as positive specificity controls. Microphotographs were taken by an Olympus BX51 microscope equipped with excitation filters for green (FITC), red (rhodamine), and blue (DAPI) fluorescence and a DP70 digital camera (Olympus Europe, Hamburg, Germany).

Statistics

One-way ANOVA, followed by Bonferroni post hoc test, was used for multiple comparisons. All analyses were performed by using SPSS Statistics software, version 17.0. Differences were considered to be statistically significant at $P < 0.05$. Significance is indicated by $*P < 0.05$; $**P < 0.01$; $***P < 0.005$.

RESULTS

Baseline expression and induction of RIG-I/MDA5 in human moDCs

The cytosolic RLR sensors RIG-I and MDA5 share dsRNA specificity with membrane TLR3, but their role in human DC biology is poorly understood. We first mapped the expression of RIG-I and MDA5 in resting moDCs and found that they express both sensors, albeit at lower levels than monocytes (**Fig. 1A** and **B**) but inducible by ATRA, LPS, and poly(I:C) (Fig. 1C–E). The results obtained with Donors 1, 2, and 3,

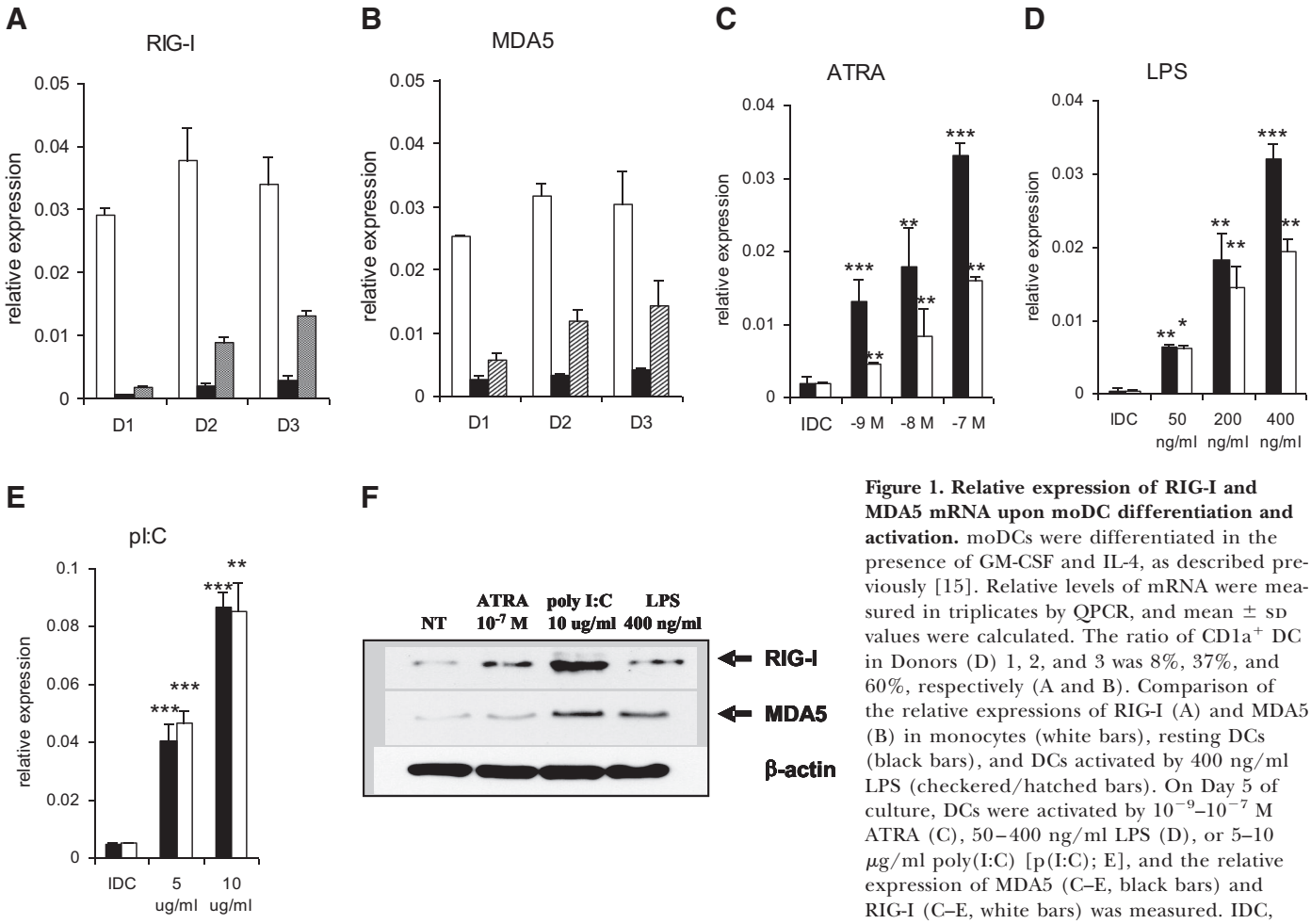

Figure 1. Relative expression of RIG-I and MDA5 mRNA upon moDC differentiation and activation. moDCs were differentiated in the presence of GM-CSF and IL-4, as described previously [15]. Relative levels of mRNA were measured in triplicates by QPCR, and mean ± SD values were calculated. The ratio of CD1a$^+$ DC in Donors (D) 1, 2, and 3 was 8%, 37%, and 60%, respectively (A and B). Comparison of the relative expressions of RIG-I (A) and MDA5 (B) in monocytes (white bars), resting DCs (black bars), and DCs activated by 400 ng/ml LPS (checkered/hatched bars). On Day 5 of culture, DCs were activated by 10^{-9}–10^{-7} M ATRA (C), 50–400 ng/ml LPS (D), or 5–10 μg/ml poly(I:C) [p(I:C); E], and the relative expression of MDA5 (C–E, black bars) and RIG-I (C–E, white bars) was measured. IDC, Immature DC. Protein expression was detected by Western blotting of cell lysates (F) prepared from nontreated (NT) or ATRA-, poly(I:C)-, or LPS-activated DCs. Representative experiments out of three to five are shown.

characterized by increasing ratios of CD1a$^+$ cells, suggested that mRNA expression of the helicases may correlate to the presence of CD1a$^+$ cells, previously indentified as PPARγ-negative DCs with the capability to produce high amounts of inflammatory cytokines and chemokines [15].

ATRA, LPS, and poly(I:C) are potent inducers of RIG-I and MDA5 expression in various cell types [19], but their activity to increase RLR expression in human moDCs has not been analyzed. Moreover, poly(I:C) is a ligand of RLRs [20] and TLR3, although endosomal TLR3 has been shown to detect endocytosed poly(I:C) [21], whereas RIG-I/MDA5 are able to sense poly(I:C) penetrating through the cell membrane by an unknown mechanism [22]. To compare the effect of these activators on moDCs, we first measured RIG-I and MDA5 mRNA expression after activation by graded doses of ATRA, poly(I:C), or LPS (Fig. 1C–E). ATRA did not result in moDC activation monitored by CD83 and CD86 expression, but LPS and poly(I:C) stimulation resulted in >80% activated cells (data not shown). Despite its inactivity to induce moDC activation, stimulation by ATRA (Fig. 1C), LPS (Fig. 1D), or poly(I:C) (Fig. 1E) induced increased RIG-I and MDA5 expression in these cells in a dose-dependent manner, detected at mRNA (Figs. 1C–E) and protein (Fig. 1F) levels, and poly(I:C) turned out to be the most potent enhancer of RLR expression. These results altogether demonstrate that besides membrane TLR3, resting moDCs also express cytosolic helicases, which can be induced by various stimuli.

Subset-dependent expression and activity of RLR-related genes in moDCs

PRRs are distributed in a cell type-specific manner, and upon stimulation by specific ligands, they may provoke collaborative or inhibitory signals [23]. To assess the expression of RIG-I and MDA5 and the components of the related signaling cascade in the moDC subsets, we sorted the cells to CD1a$^+$ and CD1a$^-$ fractions and subjected them to mRNA and protein analysis. Both resting moDC subsets were shown to express RIG-I and MDA5,

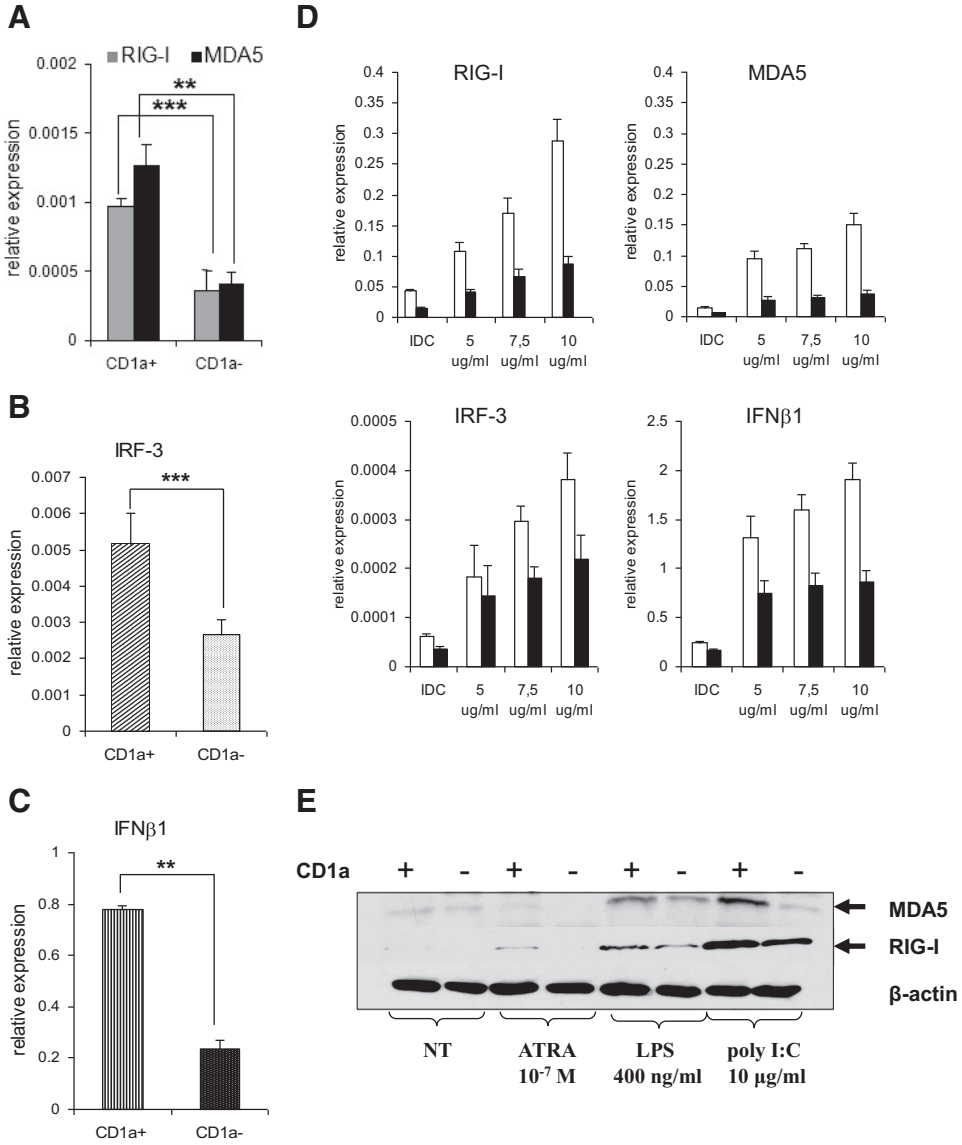

Figure 2. Expression of RLR, IRF3, and IFN-β1 genes in separated moDC subsets. The expression of RIG-I, MDA5, IRF3, and IFN-β1 genes was measured at the mRNA level in CD1a$^+$ and CD1a$^-$ cells isolated by flow cytometry before activation. (A) Comparison of relative mRNA expressions of RIG-I (gray bars) and MDA5 (black bars) in resting DCs. (B and C) Baseline expressions of IRF3 and IFN-β1 genes in CD1a$^+$ and CD1a$^-$ DCs are shown as mean ± SD of three independent experiments. (D) Expression profiles of RIG-I, MDA5, IRF3, and IFN-β1 in activated CD1a$^+$ (white bars) and CD1a$^-$ (black bars) cells. Activation of sorted cells was induced on Day 5 of culture by 5, 7.5, and 10 μg/ml poly(I:C). Mean ± SD values of three independent donors are presented. (E) Expression of RIG-I and MDA5 proteins tested by immunoblot in resting and ATRA-, LPS-, or poly(I:C)-activated CD1a$^+$ and CD1a$^-$ DCs. A representative experiment out of three is presented.

the downstream transcription factor IRF3, and the effector cytokine IFN-β1 (**Fig. 2**). Interestingly, CD1a$^+$ cells exhibited significantly higher baseline expression of RIG-I, MDA5, IRF3, and IFN-β1 genes than CD1a$^-$ cells (Figs. 2A–C). Furthermore, activation by increasing doses of poly(I:C) resulted in the coordinated up-regulation of RLR, IRF3, and IFN-β1 mRNA preferentially in CD1a$^+$ cells (Fig. 2D). Activated CD1a$^+$ moDCs also displayed higher levels of RIG-I and MDA5 proteins as compared with the CD1a$^-$ subset (Fig. 2E). Our results showed that ATRA and LPS stimulation also resulted in up-regulation of RIG-I/MDA5 expression preferentially in CD1a$^+$ cells as compared with its CD1a$^-$ counterpart (Fig. 2E); however, unlike poly(I:C), these stimuli did not show clear subset-specific differences in the enhancement of IRF3 and IFN-β1 gene expression levels (data not shown). Although ATRA up-regulated the expression of RIG-I/MDA5 genes, it failed to trigger IRF3 phosphorylation and to induce IFN-β signaling (data not shown), indicating that it does not contribute to cytokine secretion. These results demonstrate that the baseline and activation-induced expressions of RIG-I, MDA5, IRF3, and IFN-β1 genes show a significant difference in the CD1a$^+$ and CD1a$^-$ moDC subsets.

Activation of NF-κB- and IRF3-mediated signaling pathways in CD1a$^+$ and CD1a$^-$ moDCs

To determine the contribution of NF-κB and the IRF3– IFN-β signal transduction pathways in CD1a$^+$ and CD1a$^-$ moDCs, we compared the levels of pIκBα with pIRF3 (**Fig. 3A**). As a result of poly(I:C) stimulation, we detected rapid activation of both pathways and found obvious differences in IκBα and IRF3 phosphorylation levels detected in the two DC subsets. Concordant to the differential expression of RIG-I and MDA5 receptors, CD1a$^+$ and CD1a$^-$ moDCs not only differed in the expression levels of the key molecules (Fig. 2) but also in the functional activity of the downstream signaling machinery (Fig. 3A).

To assess the impact of differential helicase-mediated signaling on DC functional activity, we measured the concentration of inflammatory cytokines and chemokines secreted by activated CD1a$^+$ and CD1a$^-$ moDCs. The tested cytokines involved TNF-α, IL-6, IL-12p70, and CXCL10 as signatures of the NF-κB pathway, and IFN-β controlled by IRF3. Figure 3B shows the concentration of the secreted cytokines in a typical experiment out of nine. Comparison of the relative cytokine levels in all donors revealed statistically significant differences for IL-6 (P=0.009), TNF-α (P=0.036), IL-12p70 (P=0.002), CXCL10 (P=0.007), and IFN-β (P=0.006). These results indicate that as a result of their distinct RLR expression and signaling activity, the CD1a$^+$ and CD1a$^-$ moDC subsets participate in the inflammatory and IFN responses to different extent.

Type I IFN-β but not inflammatory cytokine production is controlled by RLR in human CD1a$^+$ moDCs

The IFN and inflammatory cytokine responses of DCs are mediated by the collaboration of multiple converging signaling pathways, which involve the NF-κB, IRF3, and AP-1 transcription factors [24]. We showed previously that upon poly(I:C) activation, the production of inflammatory cytokines and type I IFN-β is primarily attributed to CD1a$^+$ moDCs (Figs. 2 and 3). As the dsRNA

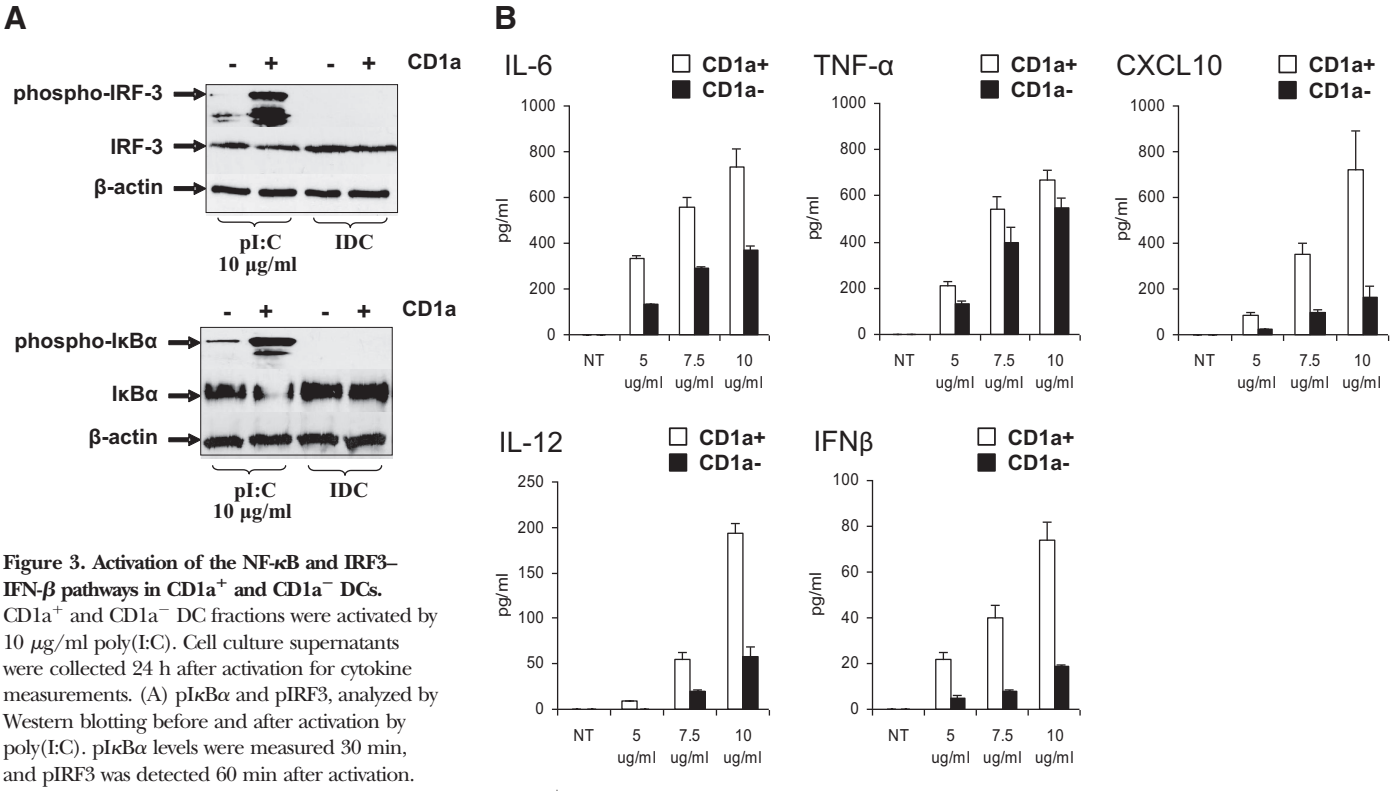

Figure 3. Activation of the NF-κB and IRF3–IFN-β pathways in CD1a$^+$ and CD1a$^-$ DCs. CD1a$^+$ and CD1a$^-$ DC fractions were activated by 10 μg/ml poly(I:C). Cell culture supernatants were collected 24 h after activation for cytokine measurements. (A) pIκBα and pIRF3, analyzed by Western blotting before and after activation by poly(I:C). pIκBα levels were measured 30 min, and pIRF3 was detected 60 min after activation. (B) Concentration of inflammatory cytokines secreted by CD1a$^+$ (white bars) and CD1a$^-$ (black bars) cells measured by ELISA. Data of a representative donor out of nine are shown.

analog poly(I:C) is a shared ligand of RLRs and TLR3, to dissect the roles of RLR- and TLR3-mediated signaling cascades, we used the siRNA technology and silenced the RLR or TLR3 genes in $CD1a^+$ cells. The efficacy of gene silencing was checked by QPCR and ELISA (Supplemental Fig. 1). Silencing of the TLR3 gene resulted in dramatic down-regulation of the secretion of proinflammatory cytokines IL-6, TNF-α, and CXCL10, known to be under the control of NF-κB (**Fig. 4A**). Interestingly, the production of these cytokines was not affected significantly when the RIG-I/MDA5 genes were down-regulated, whereas the production of IFN-β decreased significantly (Fig. 4B). These results show that upon poly(I:C) stimulation, the production of IFN-β is controlled preferentially by RLR expression and function, whereas TLR3 acts as a regulator of proinflammatory cytokine secretion in human $CD1a^+$ moDCs.

Contribution of $CD1a^-$ and $CD1a^+$ moDC subtypes to the antiviral immune response

The role of type I IFNs in priming adaptive T cell responses is well established in mice and human [25]. Type I IFNs are able to enhance T cell activity via APCs, which exert a direct effect on the autocrine and/or paracrine secretion of these IFNs [26], and influenza virus is known to activate RIG-I/MDA5 specifically [27, 28]. We hypothesized that $CD1a^+$ DCs, demonstrated to produce large amounts of IFN-β, should be more efficient than that of $CD1a^-$ cells to prime T cells in an in vitro human virus-infection model. To determine the functional relevance of DC subtype-specific regulation of IFN-β secretion, we sought to analyze the involvement of $CD1a^+$ and $CD1a^-$ moDCs in priming influenza virus-specific T lymphocyte responses. In these experiments, moDCs were infected by live or incubated with inactivated seasonal H1N1 influenza virus and then cocultured with isolated, naive $CD4^+$ or $CD8^+$ autologous T lymphocytes. Infection of DCs by live influenza virus provoked robust $CD8^+$ and lower but reproducible levels of $CD4^+$ virus-specific T cell responses, whereas the number of IFN-γ-producing $CD8^+$ T cells induced by inactivated virus remained low (**Fig. 5A**). When the autologous, naïve $CD8^+$ T cells were activated by sorted $CD1a^+$ or $CD1a^-$ DCs, activated by live virus, the number of IFN-γ-producing T cells was significantly higher in the cocultures containing $CD1a^+$ cells (Fig. 5B, white bars) as compared with cultures with $CD1a^-$ cells (Fig. 5B, black bars), underlying the preferential contribution of the $CD1a^+$ DC subset in virus-specific CTL stimulation. Silencing RIG-I/MDA5 expression in moDCs by specific siRNA resulted in 68 $\pm$ 5% (n=3) reduction in the number of IFN-γ-secreting T lymphocytes in both subsets, demonstrating the RIG-I/MDA5 dependence of the $CD8^+$ T cell response (Fig. 5C).

These results confirm the functional role of RIG-I/MDA5 and the related signaling pathway in regulating influenza virus-specific $CD8^+$ T cell activation, triggered preferentially by $CD1a^+$ moDCs. Our studies also indicate that $CD1a^+$ cells but not $CD1a^-$ DCs acquire a differentiation state, which is sensitized to the rapid activation of the RLR cascade ensured by high basal expression levels of the sensors and components of the downstream signaling pathway.

Ex vivo examination of RIG-I and MDA5 expression in human tonsil and LN DCs

moDCs have been classified as migratory and inflammatory cells, which could be indentified in peripheral tissues and LNs [29]. To analyze the tissue distribution of RIG-I/MDA5 expressing DCs, we performed IHC and IF staining of tonsil, resting, and reactive LN tissues. IP staining revealed the appearance of MDA5 (**Fig. 6B**)- and RIG-I (Fig. 6C)-expressing cells in perifollicular regions of nonreactive LNs. Double staining with S100, a typical DC marker, demonstrated that a subset of DCs was positive for RIG-I (Fig. 6D). MDA5- and RIG-I-positive DCs with typical morphology have also been detected in the interfollicular areas of reactive LNs (Figs. 6E–H). These results show that $CD1a^+$ DCs expressing RIG-I and/or MDA5 are detectable under physiological and pathological conditions and can be identified in lymphoid tissues.

DISCUSSION

Identification of DC subsets with specific functions has emerged recently as a new challenge of DC biology. DCs, developing under inflammatory conditions, support protection against pathogens, whereas DC subsets differentiating under steady state play a role in the control and resolution of inflammation and tissue destruction [30, 31]. This functional divergence is determined by the destination site of DC precursors and the subtype-specific and compartmentalized expression of PRRs. In contrast to the restricted expression of the nucleotide recognizing TLR [11], RLRs, specialized for the recognition of shorter or longer dsRNA, are present in multiple cell types [32].

In this study, we compared the expression and functional activity of RLR family members in two previously characterized human moDC subsets distinguished by the expression and activity of PPARγ, which controls the expression of type I CD1 molecules [14]. The $CD1a^+$ and $CD1a^-$ moDC subtypes were shown to differ in the uptake of apoptotic cells [16] and their potential to provoke inflammatory T lymphocyte responses [15] and have been shown to ameliorate immune pathology in influenza virus infection [18]. To assess the functional importance of $CD1a^+$ and $CD1a^-$ moDC subsets in the RLR-mediated inflammatory cytokine and type I IFN responses and their role in priming influenza virus-specific T cell responses, we performed in vitro and ex vivo experiments. Our results show that the baseline expression of RIG-I/MDA5, IRF3, and IFN-β, key elements of the downstream signaling cascade, is significantly higher in $CD1a^+$ cells than in their $CD1a^-$ counterparts. Activation of these DC subsets by specific ligands, i.e., poly(I:C) or influenza virus, revealed that the coupled signaling machinery is more active in the $CD1a^+$ moDC subset than in $CD1a^-$ cells. These results altogether show that in human moDCs, the RLR cascade acts in a subtype-specific manner. Furthermore, the results of our siRNA experiments revealed that in the inflammatory $CD1a^+$ moDC subset, the TLR3–NF-κB and RLR–IFN-β pathways control the production of different sets of cytokines and as a result of their subset-specific activity, work independently. The putative in vivo role of the $CD1a^+$ RLR-expressing DC subtype is suggested by the appearance of these cells in human tonsils and reactive LNs.

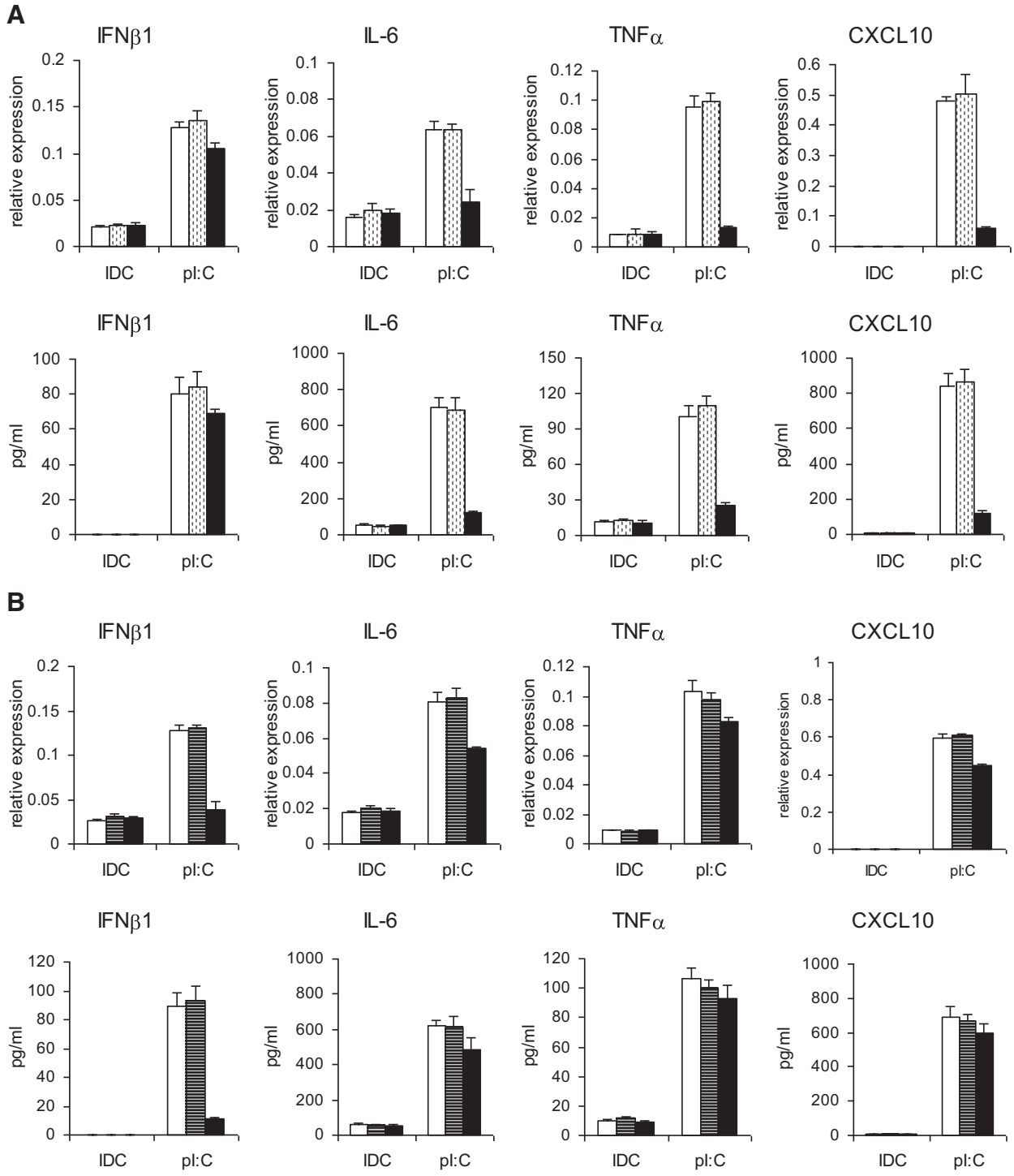

Figure 4. Functional dissection of the RLR- and TLR3-mediated signaling pathways in CD1a$^+$ moDC. moDCs were harvested on Day 3 and transfected by siRNA specific for RIG-I/MDA5 (BiMix), TLR3, or control siRNA or left untreated. Differentiated DCs were collected on Day 5, and a fraction of cells was stimulated by 10 μg/ml poly(I:C). Cell lysates of resting and activated moDCs were subjected to mRNA quantitation; supernatants of the cultures were used for cytokine measurements. (A) The effect of TLR3 siRNA treatment on mRNA expression and secreted cytokine levels before and after activation by 10 μg/ml poly(I:C). White and checkered bars represent nontreated and control siRNA-treated samples; black bars show the effect of TLR3-specific siRNA treatment. (B) The effect of RIG-I/MDA5 silencing on gene expression and secretion of cytokines in immature and poly(I:C) (10 μg/ml)-activated moDCs. White and striped bars represent nontreated and control siRNA-treated samples, whereas black bars show the effect of RLR-specific siRNA treatment. Mean ± SD values of triplicate measurements in a representative donor out of three are shown (see also Supplemental Fig. 1).

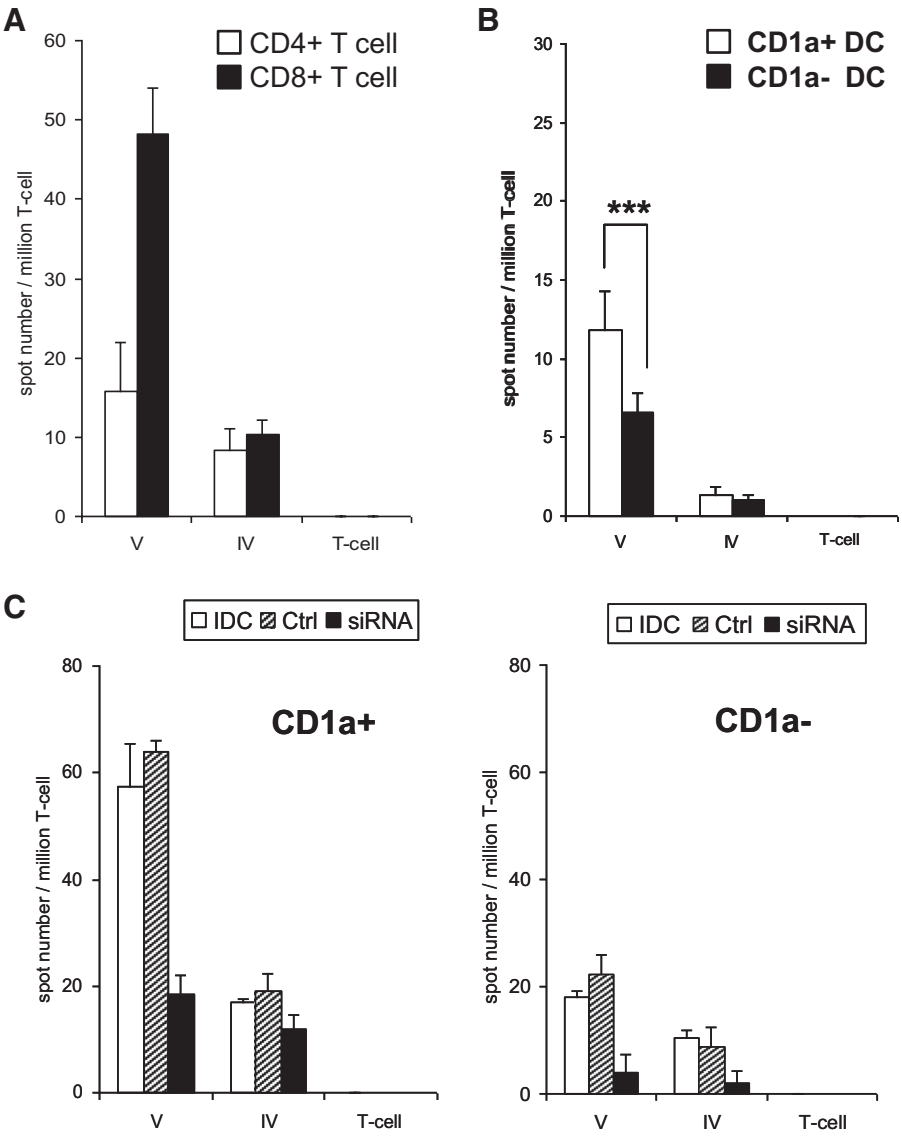

Figure 5. Role of RIG-I in triggering influenza virus-specific T lymphocyte responses. DCs were activated by influenza virus for 24 h and then cocultured with naïve, autologous $CD4^+$ or $CD8^+$ T lymphocytes for 5 days. The number of primed IFN-γ-secreting T cells was assessed by ELISPOT assay. (A) Induction of IFN-γ production by naive $CD4^+$ (white bars) and $CD8^+$ (black bars) T cells induced by $CD1a^+$ moDCs infected by live virus (V) or loaded by inactivated virus (IV). (B) T cell activation provoked by $CD1a^+$ (white bars) and $CD1a^-$ (black bars) moDCs, previously stimulated by live or inactivated influenza virus. (C) The effect of RIG-I/MDA5 silencing on the T cell response induced by $CD1a^+$ (left panel) and $CD1a^-$ (right panel) moDC subsets. Bars represent nontreated resting (immature) DCs (white bars), negative control siRNA-treated DCs (Ctrl; checkered bars), and RLR siRNA-transfected DCs (black bars). DCs were transfected by RLR-specific siRNA on Day 3, separated by flow cytometry on Day 5, activated by virus for 24 h, and then cocultured with naïve, autologous $CD8^+$ T lymphocytes and tested as described in B. A and B represent mean ± SD values of triplicate measurements of three independent donors. In C, data of a typical donor out of five are shown.

It has been shown recently that the cross-talk of human pDC and moDC subtypes is essential for optimal antiviral immune responses [33]. TLR3 and RLR have also been shown to have different yet complementary functions upon poly(I:C)-induced, virus-specific CTL responses in mice, where TLR3 was shown to be critical for priming, whereas MDA5 for supporting $CD8^+$ memory responses. Moreover, simultaneous poly(I:C) triggering of TLR3 and RLR in cDCs combined with RLR activation in NK cells is required for potent IFN-γ responses and elimination of viruses [34]. A global, quantitative proteomic approach has been used recently to demonstrate the DC subset-specific expression of TLR, NLR, and RLR and components of the related signaling cascades in murine viral infections [35]. The authors identified splenic $CD4^+$ and double-negative DCs specialized to viral recogition by RIG-I/MDA5 instead of the $CD8\alpha^+$ DC type with a cross-presenting potential. Supporting the interpretation of these authors, we also suggest that as a result of the high basal levels of the RLR sensors and the major components of the coupled signaling pathways, human $CD1a^+$ DCs exhibit a sensitized state for priming virus-specific immune responses, whereas $CD1a^-$ cells remain incompetent for these functions.

The human homologue of mouse $CD8\alpha^+$ DCs with efficient T cell priming activity has recently been identified and characterized by the expression of the C-type lectin DC, NK lectin group receptor-1/C-type lectin-like receptor 9A, the chemokine receptor XCR1, high expression of TLR3, and efficient cross-presentation [36, 37]. This DC type, also known as blood DC antigen 3, is considered as an independent lineage based on the expression of IRF8 and basic leucine zipper transcriptional factor activating transcription factor-like 3. However, this minor cell population does not express RIG-I or MDA5 [38]. Hence, we conclude that the $CD1a^+$ migratory moDC subset with the unique potential to activate IFN-β secretion and antiviral cellular immune responses is a unique human DC subset specified by high CD1a and low PPARγ expression. As the regulation of CD1a and CD1c gene and protein expression, controlled by PPARγ, is tightly linked [17], this interpretation is

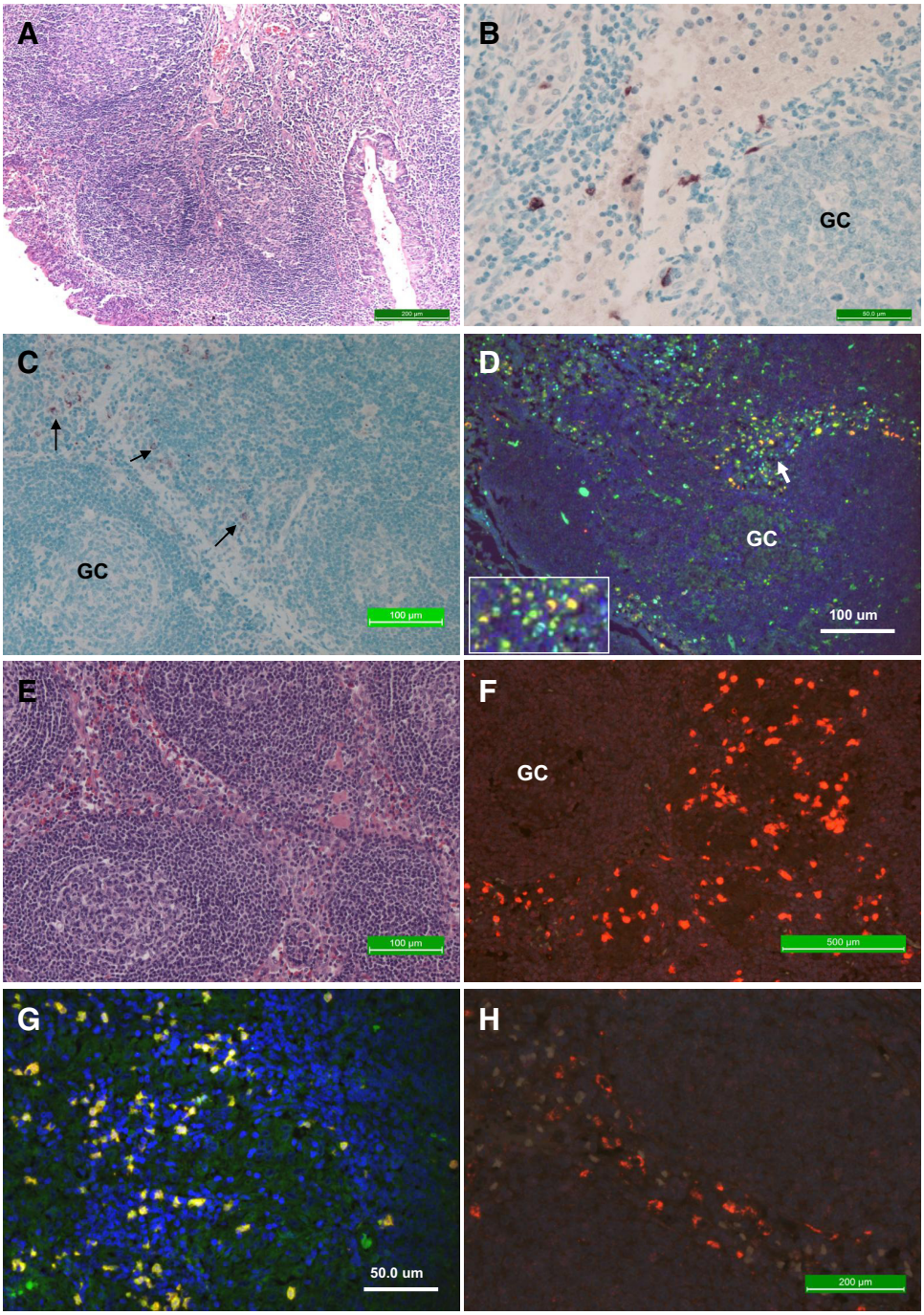

Figure 6. Immunohistological analysis of RLR expression in human tissues. (A–D) Normal tonsil. (A) hematoxylin and eosin (HE) staining (10× original); (B) IP staining for MDA5-positive cells in the perifollicular sinus system (40×original); (C) RIG-I-positive cells in the perifollicular region (20× original); (D) double IF for RIG-I (red) and S100 (green), photographed with overlay technique. The composite color, yellow fluorescence indicates DCs that express S100 and RIG-I (20× original). (E–H) Reactive LN. (E) HE (20× original); (F) perifollicular cells with cytoplamic projections that express MDA5 (20× original); (G) double IF for MDA5 (red) and S100 (green) shows DCs expressing both proteins (yellow fluorescence; 40× original); (H) interfollicular RIG-I-positive cells (red fluorescence) in part with DC morphology (40× original). (D and F–H) IF with DAPI nuclear counterstaining (blue). GC, germinal center.

supported by recent data showing that blood CD1c$^+$ DCs display the capacity of secreting high amounts of IL-12 [39].

Human CD1 proteins are closely linked to the presentation of mycobacterial lipid, glycolipid, and lipopeptide antigens for T lymphocytes [40]. Interestingly, the largest proportion of transcripts changed in *Mycobacterium tuberculosis* infection was found recently among neutrophil-dependent, IFN-inducible genes, presenting a typical signature that correlates with disease severity [41]. Thus, the expression of CD1a in human DCs marks a subset specialized for the recognition of and protection against intracellular pathogens through the elevated baseline expression of cytosolic RLR sensors and components of the coupled signaling machinery, which support type I IFN responses and polarization to inflammatory T lymphocyte differentiation.

We also showed that the increased activity of the RLR–IRF3–IFN-β signaling pathway results in efficient activation of naïve, autologous CD8$^+$ T lymphocytes by the CD1a$^+$ subset, and silencing of RIG-I/MDA5 abrogates this effect. The presence of RLR-positive DCs in human lymphoid tissues suggests the possible importance of these cells during infections. Thus, our findings not only describe the underlying mechanism of IFN-β production by moDC subsets but also identify the CD1a$^+$ DC subtype as a po-

tential target for improving the efficacy of prophylactic and/or therapeutic vaccines against intracellular pathogens.

The distinct, functional attributes of $CD1a^+$ and $CD1a^-$ moDC subsets may result in reasonable, functional complementarity based on their inflammatory and phagocytic activities. At the early stage of infection, bone marrow-derived $CCR2^+$ monocytes and moDCs and TNF-α/iNOS-producing DCs rapidly act as potent, local APCs for $CD8^+$ T cells, but upon infection by highly pathogenic influenza viruses, their recruitment correlates with immune pathology [18]. In a mouse model of influenza virus infection, the major source of IL-12 was associated to a moDC subset that enters inflamed LNs directly from the blood, guided by CCR2 [42]. In our model, we suggest that dead, infected epithelial cells can be internalized efficiently by resident, highly phagocytic but less inflammatory PPARγ-positive $CD1a^-$ DCs, which may use vesicular TLRs for the recognition of nucleotides in engulfed apoptotic cells and confer immunomodulatory effects [16]. In contrast, sensing dsRNA and triggering IFN-β responses through RIG-I and MDA5 are mediated by IL-12p70, producing inflammatory $CD1a^+$ moDCs, which are able to provoke CTL activation against viruses and other intracellular pathogens. Cheong et al. [43] have shown recently that repeated inoculation of mice with LPS results in the migration of circulating monocytes to LNs and their rapid differentiation to $DC\text{-}SIGN^+$ moDCs. As these cells act as effective APCs with strong T cell-activating capacity, they are considered as "authentic" DCs. As human moDCs are widely used in various clinical settings and considered as gold standards of DC biology, we propose that identification of human moDC subsets with specialized functions may have an important impact on designing vaccines against viruses and tumor cells.

AUTHORSHIP

A.S. designed, performed experiments, analyzed data, and wrote the manuscript. K.B. and P.G. performed flow cytometry and protein-based experiments. B.D. performed IHC experiments and wrote the manuscript. B.R., A.L., and I.J. provided guidance for the experimental design and provided valuable reagents. E.R. developed the concept and interpretation, designed the study, and wrote the manuscript.

ACKNOWLEDGMENTS

This work was supported by the Hungarian Scientific Research Grants OTKA NK-72937, NK-101538, and TÁMOP 4.2.1./B-09/1/KONV-2010-0007. We thank István Kurucz and Attila Bácsi for reviewing the manuscript and Erzsébet Nagy for her excellent technical assistance.

REFERENCES

1. Shortman, K., Naik, S. H. (2007) Steady-state and inflammatory dendritic-cell development. *Nat. Rev. Immunol.* **7,** 19–30.
2. Swiecki, M., Colonna, M. (2010) Unraveling the functions of plasmacytoid dendritic cells during viral infections, autoimmunity, and tolerance. *Immunol. Rev.* **234,** 142–162.
3. Geissmann, F., Jung, S., Littman, D. R. (2003) Blood monocytes consist of two principal subsets with distinct migratory properties. *Immunity* **19,** 71–82.
4. Ginhoux, F., Tacke, F., Angeli, V., Bogunovic, M., Loubeau, M., Dai, X. M., Stanley, E. R., Randolph, G. J., Merad, M. (2006) Langerhans cells arise from monocytes in vivo. *Nat. Immunol.* **7,** 265–273.
5. Geissmann, F., Manz, M. G., Jung, S., Sieweke, M. H., Merad, M., Ley, K. (2010) Development of monocytes, macrophages, and dendritic cells. *Science* **327,** 656–661.
6. Yona, S., Jung, S. (2010) Monocytes: subsets, origins, fates and functions. *Curr. Opin. Hematol.* **17,** 53–59.
7. Kurts, C., Robinson, B. W., Knolle, P. A. (2010) Cross-priming in health and disease. *Nat. Rev. Immunol.* **10,** 403–414.
8. Banchereau, J., Palucka, A. K. (2005) Dendritic cells as therapeutic vaccines against cancer. *Nat. Rev. Immunol.* **5,** 296–306.
9. Palucka, K., Banchereau, J., Mellman, I. (2010) Designing vaccines based on biology of human dendritic cell subsets. *Immunity* **33,** 464–478.
10. Benko, S., Magyarics, Z., Szabo, A., Rajnavolgyi, E. (2008) Dendritic cell subtypes as primary targets of vaccines: the emerging role and cross-talk of pattern recognition receptors. *Biol. Chem.* **389,** 469–485.
11. Barton, G. M., Kagan, J. C. (2009) A cell biological view of Toll-like receptor function: regulation through compartmentalization. *Nat. Rev. Immunol.* **9,** 535–542.
12. Deretic, V. (2011) Autophagy in immunity and cell-autonomous defense against intracellular microbes. *Immunol. Rev.* **240,** 92–104.
13. Medzhitov, R., Horng, T. (2009) Transcriptional control of the inflammatory response. *Nat. Rev. Immunol.* **9,** 692–703.
14. Szatmari, I., Gogolak, P., Im, J. S., Dezso, B., Rajnavolgyi, E., Nagy, L. (2004) Activation of PPARγ specifies a dendritic cell subtype capable of enhanced induction of iNKT cell expansion. *Immunity* **21,** 95–106.
15. Gogolak, P., Rethi, B., Szatmari, I., Lanyi, A., Dezso, B., Nagy, L., Rajnavolgyi, E. (2007) Differentiation of CD1a− and CD1a+ monocyte-derived dendritic cells is biased by lipid environment and PPARγ. *Blood* **109,** 643–652.
16. Majai, G., Gogolak, P., Ambrus, C., Vereb, G., Hodrea, J., Fesus, L., Rajnavolgyi, E. (2010) PPARγ modulated inflammatory response of human dendritic cell subsets to engulfed apoptotic neutrophils. *J. Leukoc. Biol.* **88,** 981–991.
17. Szatmari, I., Pap, A., Ruhl, R., Ma, J. X., Illarionov, P. A., Besra, G. S., Rajnavolgyi, E., Dezso, B., Nagy, L. (2006) PPARγ controls CD1d expression by turning on retinoic acid synthesis in developing human dendritic cells. *J. Exp. Med.* **203,** 2351–2362.
18. Aldridge J. R., Jr., Moseley, C. E., Boltz, D. A., Negovetich, N. J., Reynolds, C., Franks, J., Brown, S. A., Doherty, P. C., Webster, R. G., Thomas, P. G. (2009) TNF/iNOS-producing dendritic cells are the necessary evil of lethal influenza virus infection. *Proc. Natl. Acad. Sci. USA* **106,** 5306–5311.
19. Wang, Y., Zhang, H. X., Sun, Y. P., Liu, Z. X., Liu, X. S., Wang, L., Lu, S. Y., Kong, H., Liu, Q. L., Li, X. H., Lu, Z. Y., Chen, S. J., Chen, Z., Bao, S. S., Dai, W., Wang, Z. G. (2007) Rig-I−/− mice develop colitis associated with downregulation of G α i2. *Cell. Res.* **17,** 858–868.
20. Kato, H., Takeuchi, O., Sato, S., Yoneyama, M., Yamamoto, M., Matsui, K., Uematsu, S., Jung, A., Kawai, T., Ishii, K.J., Yamaguchi, O., Otsu, K., Tsujimura, T., Koh, C.S., Reis e Sousa, C., Matsuura, Y., Fujita, T., Akira, S. (2006) Differential roles of MDA5 and RIG-I helicases in the recognition of RNA viruses. *Nature* **441,** 101–105.
21. Matsumoto, M., Seya, T. (2008) TLR3: interferon induction by double-stranded RNA including poly(I:C). *Adv. Drug Deliv. Rev.* **60,** 805–812.
22. Wang, Y., Cella, M., Gilfillan, S., Colonna, M. (2010) Cutting edge: polyinosinic:polycytidylic acid boosts the generation of memory CD8 T cells through melanoma differentiation-associated protein 5 expressed in stromal cells. *J. Immunol.* **184,** 2751–2755.
23. Kumagai, Y., Akira, S. (2010) Identification and functions of pattern-recognition receptors. *J. Allergy Clin. Immunol.* **125,** 985–992.
24. Joffre, O., Nolte, M.A., Sporri, R., Reis e Sousa, C. (2009) Inflammatory signals in dendritic cell activation and the induction of adaptive immunity. *Immunol. Rev.* **227,** 234–247.
25. Pace, L., Vitale, S., Dettori, B., Palombi, C., La Sorsa, V., Belardelli, F., Proietti, E., Doria, G. (2010) APC activation by IFN-α decreases regulatory T cell and enhances Th cell functions. *J. Immunol.* **184,** 5969–5979.
26. Huber, J. P., Farrar, J. D. (2011) Regulation of effector and memory T-cell functions by type I interferon. *Immunology* **132,** 466–474.
27. Rehwinkel, J., Tan, C. P., Goubau, D., Schulz, O., Pichlmair, A., Bier, K., Robb, N., Vreede, F., Barclay, W., Fodor, E., Reis e Sousa, C. (2010) RIG-I detects viral genomic RNA during negative-strand RNA virus infection. *Cell* **140,** 397–408.
28. Siren, J., Imaizumi, T., Sarkar, D., Pietila, T., Noah, D. L., Lin, R., Hiscott, J., Krug, R. M., Fisher, P. B., Julkunen, I., Matikainen, S. (2006) Retinoic acid inducible gene-I and MDA-5 are involved in influenza A virus-induced expression of antiviral cytokines. *Microbes Infect.* **8,** 2013–2020.
29. Jeras, M., Bergant, M., Repnik, U. (2005) In vitro preparation and functional assessment of human monocyte-derived dendritic cells—potential antigen-specific modulators of in vivo immune responses. *Transpl. Immunol.* **14,** 231–244.
30. Heath, W. R., Carbone, F. R. (2009) Dendritic cell subsets in primary and secondary T cell responses at body surfaces. *Nat. Immunol.* **10,** 1237–1244.
31. Merad, M., Manz, M. G. (2009) Dendritic cell homeostasis. *Blood* **113,** 3418–3427.
32. Takeuchi, O., Akira, S. (2008) MDA5/RIG-I and virus recognition. *Curr. Opin. Immunol.* **20,** 17–22.

33. Kramer, M., Schulte, B. M., Eleveld-Trancikova, D., van Hout-Kuijer, M., Toonen, L. W., Tel, J., de Vries, I. J., van Kuppeveld, F. J., Jansen, B. J., Adema, G. J. (2010) Cross-talk between human dendritic cell subsets influences expression of RNA sensors and inhibits picornavirus infection. *J. Innate Immun.* **2,** 360–370.
34. Perrot, I., Deauvieau, F., Massacrier, C., Hughes, N., Garrone, P., Durand, I., Demaria, O., Viaud, N., Gauthier, L., Blery, M., Bonnefoy-Berard, N., Morel, Y., Tschopp, J., Alexopoulou, L., Trinchieri, G., Paturel, C., Caux, C. (2010) TLR3 and Rig-like receptor on myeloid dendritic cells and Rig-like receptor on human NK cells are both mandatory for production of IFN-γ in response to double-stranded RNA. *J. Immunol.* **185,** 2080–2088.
35. Luber, C. A., Cox, J., Lauterbach, H., Fancke, B., Selbach, M., Tschopp, J., Akira, S., Wiegand, M., Hochrein, H., O'Keeffe, M., Mann, M. (2010) Quantitative proteomics reveals subset-specific viral recognition in dendritic cells. *Immunity* **32,** 279–289.
36. Bachem, A., Guttler, S., Hartung, E., Ebstein, F., Schaefer, M., Tannert, A., Salama, A., Movassaghi, K., Opitz, C., Mages, H. W., Henn, V., Kloetzel, P. M., Gurka, S., Kroczek, R. A. (2010) Superior antigen cross-presentation and XCR1 expression define human CD11c+CD141+ cells as homologues of mouse CD8+ dendritic cells. *J. Exp. Med.* **207,** 1273–1281.
37. Poulin, L. F., Salio, M., Griessinger, E., Anjos-Afonso, F., Craciun, L., Chen, J. L., Keller, A. M., Joffre, O., Zelenay, S., Nye, E., Le Moine, A., Faure, F., Donckier, V., Sancho, D., Cerundolo, V., Bonnet, D., Reis e Sousa, C. (2010) Characterization of human DNGR-1+ BDCA3+ leukocytes as putative equivalents of mouse CD8α+ dendritic cells. *J. Exp. Med.* **207,** 1261–1271.
38. Hildner, K., Edelson, B. T., Purtha, W. E., Diamond, M., Matsushita, H., Kohyama, M., Calderon, B., Schraml, B. U., Unanue, E. R., Diamond, M. S., Schreiber, R. D., Murphy, T. L., Murphy, K. M. (2008) Batf3 deficiency reveals a critical role for CD8α+ dendritic cells in cytotoxic T cell immunity. *Science* **322,** 1097–1100.
39. Jongbloed, S. L., Kassianos, A. J., McDonald, K. J., Clark, G. J., Ju, X., Angel, C. E., Chen, C. J., Dunbar, P. R., Wadley, R. B., Jeet, V., Vulink, A. J., Hart, D. N., Radford, K. J. (2010) Human CD141+ (BDCA-3)+ dendritic cells (DCs) represent a unique myeloid DC subset that cross-presents necrotic cell antigens. *J. Exp. Med.* **207,** 1247–1260.
40. Felio, K., Nguyen, H., Dascher, C. C., Choi, H. J., Li, S., Zimmer, M. I., Colmone, A., Moody, D. B., Brenner, M. B., Wang, C. R. (2009) CD1-restricted adaptive immune responses to *Mycobacteria* in human group 1 CD1 transgenic mice. *J. Exp. Med.* **206,** 2497–2509.
41. Berry, M. P., Graham, C. M., McNab, F. W., Xu, Z., Bloch, S. A., Oni, T., Wilkinson, K. A., Banchereau, R., Skinner, J., Wilkinson, R. J., Quinn, C., Blankenship, D., Dhawan, R., Cush, J. J., Mejias, A., Ramilo, O., Kon, O. M., Pascual, V., Banchereau, J., Chaussabel, D., O'Garra, A. (2010) An interferon-inducible neutrophil-driven blood transcriptional signature in human tuberculosis. *Nature* **466,** 973–977.
42. Nakano, H., Lin, K. L., Yanagita, M., Charbonneau, C., Cook, D. N., Kakiuchi, T., Gunn, M. D. (2009) Blood-derived inflammatory dendritic cells in lymph nodes stimulate acute T helper type 1 immune responses. *Nat. Immunol.* **10,** 394–402.
43. Cheong, C., Matos, I., Choi, J. H., Dandamudi, D. B., Shrestha, E., Longhi, M. P., Jeffrey, K. L., Anthony, R. M., Kluger, C., Nchinda, G., Koh, H., Rodriguez, A., Idoyaga, J., Pack, M., Velinzon, K., Park, C. G., Steinman, R. M. (2010) Microbial stimulation fully differentiates monocytes to DC-SIGN/CD209(+) dendritic cells for immune T cell areas. *Cell* **143,** 416–429.

KEY WORDS:
innate immunity · RIG-I-like receptor · inflammatory cytokine · influenza